Reactivity of Gaseous XeF^+ Ions with Acetonitrile. A Joint Mass Spectrometric and Theoretical Study of Isomeric $C_2H_3NF^+$ and $C_2H_3NXe^+$ Cations

Marina Attinà,*,† Fulvio Cacace,‡ Antonella Cartoni,† and Marzio Rosi§

Dipartimento di Scienze e Tecnologie Chimiche, Università di Roma "Tor Vergata", Via della Ricerca Scientifica, I-00133 Roma, Italy, Dipartimento di Studi di Chimica e Tecnologia delle Sostanze Biologicamente Attive, Università di Roma "La Sapienza", P.le Aldo Moro 5, I-00185 Roma, Italy, and Istituto per le Tecnologie Chimiche, Università di Perugia, Via G.Duranti, I-06125 Perugia, Italy

Received: May 17, 2000

The gas-phase reactivity of XeF^+ toward a model nucleophile, acetonitrile, was investigated by the joint application of experimental and theoretical methods. The results of mass spectrometric experiments and theoretical calculations up to the B3LYP/CCSD(T) level of theory show that XeF^+ promotes both F^+ and Xe^+ transfer to CH_3CN. Both processes involve the preliminary association of the reactants to yield two ion−molecule complexes, $[CH_3CNFXe]^+$ and $[CH_3CNXeF]^+$, of comparable stability. The former can undergo Xe loss, yielding CH_3CNF^+, which can consequently rearrange into the CH_2FCNH^+ isomer, more stable by 263.6 kJ mol^{-1} at the CCSD(T) level of theory. The isomerization can proceed by two independent pathways and requires the overcoming of significant barriers computed to be 147.3 and 187.0 kJ mol^{-1} at the same level of theory. The CH_3CNF^+ cation reacts with typical nucleophiles (CH_3COCH_3, C_2H_4, 1,1-$C_2H_2F_2$, CH_3-OH, C_6H_6) according to three processes, i.e., charge exchange, F^+ transfer, and ion−molecule complex formation, whose relative efficiency and thermochemistry were investigated. The formation of CH_3CNXe^+ occurs via the loss of F from the primary ion−neutral complex $[CH_3CNXeF]^+$. The gas-phase reactivity of XeF^+ is discussed in comparison with the fluorination of unsaturated molecules by XeF_2 in solution.

Introduction

In sharp contrast with other electrophilic reactions, such as chlorination and nitration, cationic fluorination has been the subject of few mechanistic studies in solution. This reflects, rather than the lack of fundamental or synthetic interest, the scarcity of fluorinating electrophiles whose reactivity is not affected by the incursion of competitive, frequently overwhelming, homolitic processes. In the gas phase, the direct detection of charged reagents, intermediates, and products allowed by mass spectrometric approaches holds the promise of a sharper mechanistic discrimination. However, despite the tremendous advances in positive ion chemistry, the study of electrophilic fluorination has again been prevented by the lack of gaseous reagents capable of promoting F^+-transfer processes.

In view of the interest attached to the reactivity of the most simple halogen cation, we have undertaken a systematic search for a suitable gaseous reagent. Recently, we focused attention on XeF^+, whose role as a potentially useful fluorinating species was suggested by studies performed in solution, showing that the presence of Lewis acids enhances the fluorinating ability of XeF_2, most likely through the formation of saltlike adducts, e.g., $(XeF)^+(AsF_6)^-$ or $(XeF)^+(RuF_6)^-$.[1,2]

Accordingly, we have examined, by the joint application of mass spectrometric and theoretical methods, the gas-phase reactivity of XeF^+ with prototypical unsatured hydrocarbons. The results showed that, indeed, XeF^+ is capable of promoting efficient F^+ transfer, revealing, in addition, another interesting fact about its reactivity, namely, the ability to also undergo Xe^+ transfer to olefins.[3,4]

Herein, we describe the extension of the study to the reactions of XeF^+ with a different nucleophile, CH_3CN, containing a C−N multiple bond, to ascertain whether cationic fluorination of the N atom would occur, leading to the formation of a N−F bond. We also discuss the relative efficiency of the competitive Xe^+ transfer, leading to the formation of a N−Xe bond, very few examples of which have been reported. Acetonitrile was selected because it is a simple nucleophile whose positive-ion chemistry is well-known, and also because its reactions with a model halogenating cation are potentially relevant to areas such as atmospheric, planetary, and space chemistry, given the ubiquitous presence of CH_3CN.[5−10]

Experimental Results

Reactions of XeF^+ with CH_3CN. The charged reagent is a major ion in the CI of neat XeF_2, where its intensity reaches ca. 70% at 0.1 Torr, with smaller amounts of Xe^+ and XeF_2^+.[4] Addition of CH_3CN causes the formation of CH_3CNH^+, m/z = 42 (ca. 30%); CH_3CNF^+, m/z = 60, (ca. 40%); the CH_3CNXe^+ multiplet, m/z from 169 to 177 (cumulative intensity ca. 8%); and the CH_3CNXeF^+ multiplet, m/z from 188 to 196 (cumulative intensity ca. 20%). The reactions of mass-selected ions, e.g., the $^{129}XeF^+$ isotopomer, with acetonitrile were examined in the pressure range up to 1.1×10^{-5} Torr in the RF-only hexapolar cell of the triple quadrupole spectrometer. At such low pressures

* Author to whom correspondence should be adressed. E-mail: attina@uniroma2.it.
† Università di Roma "Tor Vergata".
‡ Università di Roma "La Sapienza".
§ Università di Perugia.

10.1021/jp001823d CCC: $19.00
Published on Web 07/20/2000

no adduct is formed, the two major reactions observed being

$$XeF^+ + CH_3CN \rightarrow C_2H_3NF^+ + Xe \quad (1)$$

$$XeF^+ + CH_3CN \rightarrow C_2H_3NXe^+ + F \quad (2)$$

A minor secondary product is CH_3CNH^+, arising from the protonation of acetonitrile by the $CH_3CN^{\bullet+}$ radical cation, which is formed, in turn, by charge-exchange processes, e.g., involving Xe^+, as shown by control experiments. As the CH_3CN pressure is increased, one observes a monotonic decrease in XeF^+, down from 100 to 50% at 1.1×10^{-5} Torr, and a parallel increase in the CH_3CNF^+ and CH_3CNH^+ products, whose intensities reach ca. 40% and 10%, respectively. Instead, the intensities of Xe^+ and CH_3CNXe^+ tend to level off, increasing to 5% and 10% at a CH_3CN pressure of 6×10^{-5} Torr and undergoing no further increase at higher pressures.

Structural Study of the Reaction Products. The structure, more properly the connectivity, of the charged products was investigated utilizing collisionally activated dissociation (CAD) spectrometry and reactive probing, based on the study of the reactivity of the species of interest with suitable nucleophiles. In the following paragraphs, the results of the two sets of experiments will be examined in some detail.

$C_2H_3NF^+$ Ions. As for all other species investigated, the ions $C_2H_3NF^+$ were obtained by ionization of a XeF_2/CH_3CN mixture in the CI source, as were $C_2D_3NF^+$ ions from d_3-acetonitrile. They were then mass selected and allowed to collide with argon at pressures from 10^{-6} to 10^{-5} Torr and center-of-mass energies up to 34 eV. The CAD spectra of the $C_2H_3NF^+$ ions assayed were compared with those of model ions with $H_2FC-CNH^+$ connectivity prepared upon protonation of fluoroacetonitrile, whose only charged fragment is, as expected, the CH_2F^+ ion at $m/z = 33$. The $C_2H_3NF^+$ ionic population from $CI/XeF_2/CH_3CN$ undergoes dissociation into CH_2F^+ ($m/z = 33$) and CH_3^+ ($m/z = 15$). From the relative intensities of the fragments, it appears that the species with H_3C-CNF^+ connectivity predominates in the $[C_2H_3NF]^+$ population sampled. Analogous results were obtained in confirmatory experiments involving CD_3CN, where CD_3^+ and CD_2F^+ ions at $m/z = 18$ and 35, respectively, were detected at relative intensities comparable to those from the unlabeled isotopomer. Independent evidence on the connectivity of the $[C_2H_3NF]^+$ population was obtained by reactive probing, utilizing the following processes:

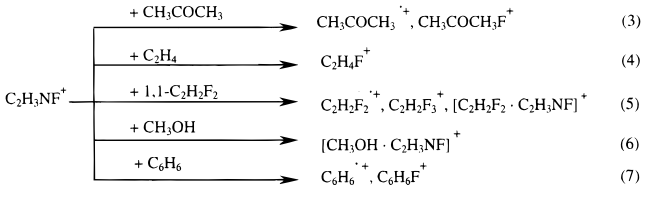

In addition to charge exchange with nucleophiles of low ionization potential (IP), e.g., reactions 3 and 7, and formation of charged complexes, e.g., reactions 5 and 6, the salient feature of the $C_2H_3NF^+$ reactivity is the fluorinating ability displayed toward acetone, ethylene, 1,1-difluoroethylene, and benzene. Formal F^+ transfer is consistent with $CH_3-C-N-F^+$ connectivity, but not with $CH_2F-C-NH^+$ connectivity, as confirmed by comparison with the model ion $CH_2F-C-NH^+$ obtained from the protonation of fluoroacetonitrile, which is devoid of fluorinating ability and reacts exclusively as a Brønsted acid.

CH_3CNXe^+ Ions. The CAD spectra display only the Xe^+ fragment, whereas the results of reactive probing experiments involving the same nucleophiles utilized in the case of $C_2H_3NF^+$ show that CH_3CNXe^+ undergoes only charge transfer to acetone, 1,1-difluoroethylene, and benzene, acting as a Xe^+ donor to ethylene and methanol.

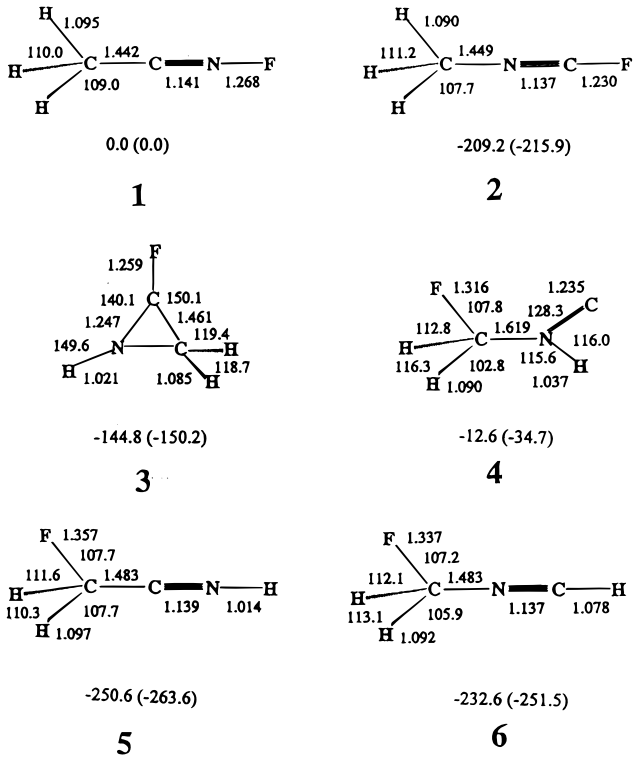

Figure 1. Optimized geometries of some relevant minima localized on the $[C_2, H_3, N, F]^+$ potential energy surface. Only the main geometrical parameters are shown for clarity. In this and in the following figures, bond lengths are in Å and angles in degrees.[20] Relative energies (kJ mol^{-1}), with respect to species **1**, evaluated at 298 K at the B3LYP (CCSD(T)) level are reported.

$[CH_3CNXeF]^+$ Ions. The CAD spectra display XeF^+ and $C_2H_3NF^+$ fragments. The ion reacts exclusively as a fluorinating agent with ethylene, 1,1-difluoroethylene, and benzene, whereas it undergoes both F^+ and XeF^+ transfer to acetone and methanol.

Theoretical Results

Methods. Density functional theory, using the hybrid[11] B3LYP functional,[12] has been used to localize the stationary points of the investigated systems and to evaluate the vibrational frequencies. Single-point energy calculations at the optimized geometries were performed using the coupled-cluster single- and double-excitation method,[13] with a perturbational estimate of the triple excitations [CCSD(T)] approach.[14] Transition states are located using the synchronous transit-guided quasi-Newton method due to Schlegel and co-workers.[15] The 6-311G(d,p) basis set[16] was used for all atoms except xenon. Xenon was described with a relativistic effective potential (including a spin−orbit potential) that leaves the d subshell in the valence space, resulting in 18 valence electrons.[17] The basis set reported in ref 17 was used for xenon in a decontracted form. Many compounds of xenon have recently been described through this technique.[18]

Zero-point energy corrections evaluated at the B3LYP level were added to the CCSD(T) energies. The 0 K total energies of the species of interest were corrected to 298 K by adding translational, rotational, and vibrational contributions. The absolute entropies were calculated by using standard statistical-mechanistics procedures from scaled harmonic frequencies and

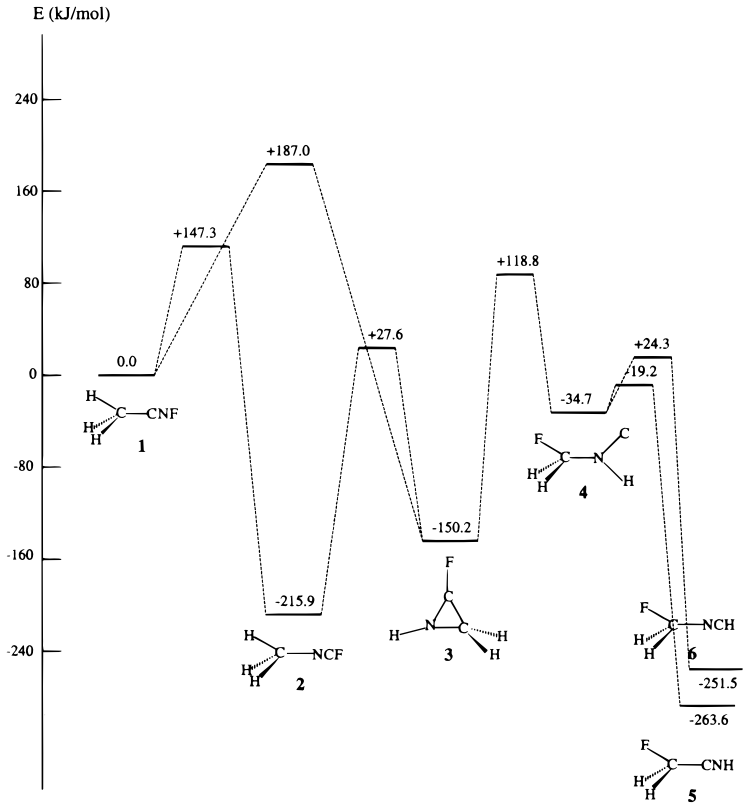

Figure 2. Energy profile surface for the isomerization of $[CH_3CNF]^+$ to $[CH_2FCNH]^+$. Relative energies (kJ mol^{-1}), with respect to species **1**, evaluated at 298 K at the CCSD(T) level are shown.

moments of inertia relative to B3LYP-optimized geometries. All calculations were performed using Gaussian 98.[19]

Results

Figure 1 shows the optimized structure and the relative energies evaluated at 298 K, at both the B3LYP and CCSD(T) levels, of several isomers of $C_2H_3NF^+$. In particular, we have examined the isomerization of **1**, the primary species derived from the attack of F^+ to acetonitrile,[20] to **5**, the most stable isomer of $C_2H_3NF^+$. The transition states connecting the minima of Figure 1 were also evaluated, together with their relative energies computed with respect to species **1**.[20] Two possible pathways from **1** to **5** have been found on the $[C_2, H_3, N, F]^+$ potential energy surface, as reported in Figure 2. **1** can isomerize directly to **3**, overcoming a barrier of 187.0 kJ mol^{-1} at the CCSD(T) level of theory, or it can isomerize first to **2** through a barrier of 147.3 kJ mol^{-1}. The isomerization of **2** into **3** requires that a barrier of 243.5 kJ mol^{-1} be overcome. Ion **3** then isomerizes to **4** (energy barrier of 269.0 kJ mol^{-1}), and the latter can evolve into **5** or **6** through lower barriers. The enthalpy changes and the energy barriers computed at 298 K at both the B3LYP and CCSD(T) levels of theory are reported in Table 1 for all of the investigated processes. Table 2 shows thermochemical data, computed at both levels of calculation, for selected reactions of species **1** and **5**. One can notice that **1** is able to transfer F^+ to C_2H_4, $C_2F_2H_2$, and C_6H_6, which is not the case for **5**. This points to **1** as the primary species produced, as the energetically allowed reactions are all experimentally observed. From Table 2, one can also see that **1** is expected to react with acetone mainly by charge transfer. The dissociation of **1** into CH_3^+ and CNF and that of **5** into HNC and CH_2F^+ are both endothermic processes, the latter being considerably less unfavorable.

TABLE 1: Energy Changes and Barrier Heights (kJ mol^{-1}, 298 K) Computed at the B3LYP (CCSD(T)) Level of Theory for the Isomerization Processes of $[CH_3CNF]^+$

process	$\Delta H°$	barrier height
1 → **2**	−209.2 (−215.9)	+142.7 (+147.3)
1 → **3**	−144.8 (−150.2)	+190.0 (+187.0)
2 → **3**	+64.4 (+65.7)	+241.4 (+243.5)
3 → **4**	+132.2 (+115.5)	+264.0 (+269.0)
4 → **5**	−238.0 (−228.9)	+5.9 (+15.5)
4 → **6**	−220.0 (−216.8)	+57.3 (+59.0)

The optimized geometry of $[CH_3CNFXe]^+$ is shown in Figure 3. This species can be seen as an electrostatic complex of Xe and CH_3CNF^+, as suggested by the very long F−Xe bond and the other geometrical parameters, close to those of free CH_3CNF^+, and by the very low bond energy between Xe and CH_3CNF^+, as reported in Table 3. Figure 3 also shows the geometry of the other isomer, $[CH_3CNXeF]^+$, and of the CH_3CNXe^+ ion. $[CH_3CNXeF]^+$ is very close in energy to $[CH_3CNFXe]^+$, being less stable by only 9.6 kJ mol^{-1} at the CCSD(T) level of theory. Intramolecular isomerization of these two species would imply, however, the overcoming of a 147.7 kJ mol^{-1} barrier of at the CCSD(T) level of calculation.[20] The data reported in Table 3 suggest that the reaction between CH_3CN and XeF^+ can lead both to $[CH_3CNFXe]^+$ and to $[CH_3CNXeF]^+$. The first species easily undergoes Xe loss, giving CH_3CNF^+, whereas the second can react with several nucleophiles, as suggested by the data reported in Table 3. Finally, the reaction of **1** with CH_3OH does not imply F^+ transfer, but preferably formation of complex **10**, whose structure is shown in Figure 3.

Discussion

The two reaction sequences promoted by the gas-phase interaction of XeF^+ with acetonitrile, eventually resulting in F^+

TABLE 2: Relevant Thermochemical Data (kJ mol^{-1}, 298 K) Computed at the B3LYP (CCSD(T)) Level of Theory for $[CH_3CNF]^+$

process	$\Delta H°$	$\Delta G°$
1 + $C_2H_4 \rightarrow CH_3CN + C_2H_4F^+$	−146.9 (−161.5)	−145.6 (−162.3)
5 + $C_2H_4 \rightarrow CH_3CN + C_2H_4F^+$	+104.2 (+102.1)	+104.6 (+102.5)
1 + $CH_3OH \rightarrow CH_3CN + CH_3OHF^+$	+88.3 (+74.1)	+89.5 (+ 75.3)
1 + $CH_3OH \rightarrow CH_3OH$- -$FNCCH_3^+$	−128.4 (−133.5)	−80.3 (−85.4)
1 + $C_2F_2H_2 \rightarrow CH_3CN + C_2F_3H_2^+$	−205.9 (−228.4)	−206.3 (−228.9)
5 + $C_2F_2H_2 \rightarrow CH_3CN + C_2F_3H_2^+$	+44.8 (+35.1)	+46.0 (+36.0)
1 + $C_6H_6 \rightarrow CH_3CN + C_6H_6F^+$	−255.2 (−260.7)	−259.4 (−265.3)
5 + $C_6H_6 \rightarrow CH_3CN + C_6H_6F^+$	−4.6 (+2.5)	−7.1 (−0.4)
1 + $CH_3COCH_3 \rightarrow CH_3CN + CH_3COCH_3F^+$	−14.2 (−13.8)	−7.9 (−7.5)
1 + $CH_3COCH_3 \rightarrow CH_3CNF + CH_3COCH_3^+$	−73.6 (−63.2)	−77.8 (−67.8)
1 $\rightarrow CNF + CH_3^+$	+412.5 (+392.5)	+369.0 (+348.9)
1 $\rightarrow NCF + CH_3^+$	+123.8 (+102.1)	+83.3 (+61.9)
5 $\rightarrow CH_2F^+ + HNC$	+304.2 (+291.2)	+263.2 (+247.7)
5 $\rightarrow CH_2F^+ + HCN$	+246.0 (+227.6)	+203.8 (185.3)

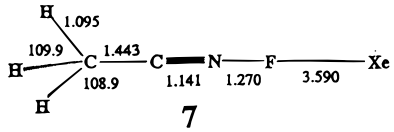

7

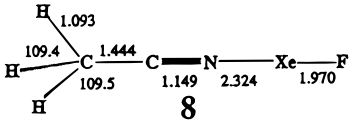

8

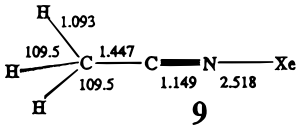

9

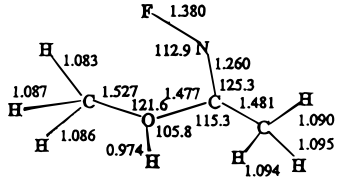

10

Figure 3. Optimized geometries of the species $[CH_3CNFXe]^+$, $[CH_3CNXeF]^+$, and $[CH_3CNXe]^+$, and of the $[CH_3CNF{\cdot}CH_3OH]^+$ adduct.

and Xe^+ transfer, as well as the structural and energetic features of the products, are discussed below, through a combination of the experimental and theoretical pieces of evidence reported in the previous sections.

Association of the Reagents. Formation of the complexes **7** and **8** is strongly exothermic, involving $\Delta H°$ values of −190.8 and − 181.2 kJ mol^{-1}, respectively, according to the results of the CCSD(T) calculations (Table 3). [Note that the CCSD(T) results will be utilized throughout the present discussion.] Formation of ions whose *m*/*z* ratios correspond to those of **7** and **8** is experimentally observed only in the high-pressure CI source, where collisional deactivation allows partial stabilization of the adducts, which are highly excited by the exothermicity of their formation process and hence prone to back dissociation or evolution into the products. The CAD spectra of the adducts population display fragments from the loss of Xe, a process consistent with the $H_3C-CN-F-Xe$ connectivity of **7**, and from the loss of CH_3CN, consistent with the connectivities of both **7** and **8**. The results of reactive probing experiments, demonstrating the ability of the adducts sampled to undergo both F^+ and XeF^+ transfer to gaseous nucleophiles, are also consistent with the connectivities of both **7** and **8**. In summary, on the basis of the combined mass spectrometric and theoretical evidence, the association of XeF^+ and CH_3CN is likely to yield a mixed population of complexes **7** and **8**, whose intramolecular interconversion requires the overcoming of a barrier, 147.7 kJ mol^{-1} at the CCSD(T) level of calculation, that is lower than the energy released in the formation of the adducts. Neverthless, the most likely pathway of **7** $\rightleftarrows$ **8** isomerization is back dissociation and reassociation of the costituent units.

The Fluorination Process and Its Products. The theoretical results identify the slightly endothermic dissociation

$$\underset{\mathbf{1}}{H_3C-CNF-Xe^+} \rightarrow \underset{\mathbf{1}}{H_3C-CNF^+} + Xe \qquad (8)$$

as the source of cation **1**, characterized by the $H_3C-C-N-F$ connectivity (Table 3). The subsequent course of the reaction, and its implications for the structure of the $C_2H_3NF^+$ fluorinated products, can be summarized as follows.

The fraction of the ionic population from reaction 8 that is collisionally deactivated retains the original structure **1**, consistent with the detection of the CH_3^+ fragment in its CAD spectrum and with its fluorinating ability, demonstrated by the reactive probing experiments. In this connection, the computed thermochemical data of Table 2 show that ion **1**, but not ion **5**, can promote exothermic F^+ transfer to C_2H_4, 1,1-$C_2H_2F_2$, and C_6H_6, all experimentally demonstrated processes.

On the other hand, the fraction of ions **1** that contain excess internal energy can isomerize to **5** following two alternative pathways. The path involving the intermediacy of **3** and **4** requires ions **1** to overcome a barrier of 187.0 kJ mol^{-1}, which is high, but comparable to the overall exothermicity of their formation process. The pathway involving the intermediacy of **2**, **3**, and **4** requires, instead, that ions **1** overcome a barrier of 147.3 kJ mol^{-1}. Once ion **1** has overcome the above-mentioned, relatively high barriers, the two isomerization sequences to **5** are energetically downhill, being characterized by lower barriers. Formation of **5**, the most stable end product, is favored over that of **6**, that requires the precursor **4** to overcome a barrier computed to be 43.5 kJ mol^{-1} higher at the CCSD(T) level of theory. The theoretical description of the isomerization process is consistent with the experimental features reported in the previous sections.

The Xe^+-Transfer Process. The source of the experimentally observed $C_2H_3NXe^+$ ions is traced to the dissociation process

$$\underset{\mathbf{8}}{H_3CCNXeF^+} \rightarrow \underset{\mathbf{9}}{H_3CCNXe^+} + F \qquad (9)$$

which is computed to be endothermic by 128.9 kJ mol^{-1} at the

TABLE 3: Relevant Enthalpy Changes (kJ mol^{-1}, 298 K) Computed at the B3LYP and CCSD(T) Levels of Theory for the Systems Containing Xenon

process	B3LYP	CCSD(T)
$CH_3CN + XeF^+ \rightarrow CH_3CNF^+ + Xe$	−193.3	−187.9
$CH_3CN + XeF^+ \rightarrow CH_3CNXe^+ + F$	−41.4	−52.3
$CH_3CN + XeF^+ \rightarrow CH_3CNXeF^+$	−221.8	−181.2
$CH_3CNXeF^+ \rightarrow CH_3CNFXe^+$	−196.2	−190.8
$CH_3CNXeF^+ \rightarrow CH_3CNXe^+ + F$	+179.9	+128.9
$CH_3CNFXe^+ \rightarrow CH_3CNF^+ + Xe$	+5.4	+5.4
$CH_3CNXeF^+ + CH_3COCH_3 \rightarrow CH_3CNXe + CH_3COCH_3F^+$	+15.1	−19.7
$CH_3CNXeF^+ + CH_3COCH_3 \rightarrow CH_3CN + CH_3COCH_3$- -$XeF^+$	−5.9	−4.2
$CH_3CNXeF^+ + C_2H_4 \rightarrow CH_3CNXe + C_2H_4F^+$	−117.2	−167.4
$CH_3CNXeF^+ + C_2F_2H_2 \rightarrow CH_3CNXe + C_2F_3H_2^+$	−146.1	−234.3
$CH_3CNXeF^+ + CH_3OH \rightarrow CH_3CNXe + CH_3OHF^+$	+118.0	+68.2
$CH_3CNXeF^+ + CH_3OH \rightarrow CH_3CN + CH_3OH$- -$XeF^+$	+48.5	+47.3
$CH_3CNXeF^+ + C_6H_6 \rightarrow CH_3CNXe + C_6H_6F^+$	−225.5	−266.9
$CH_3CNXe^+ + C_2H_4 \rightarrow CH_3CN + C_2H_4Xe^+$	−43.5	−26.8
$CH_3CNXe^+ + CH_3OH \rightarrow CH_3CN + CH_3OHXe^+$	−31.4	+34.3

CCSD(T) level of theory (Table 3). Despite its significant endothermicity, process 9 is accessible to ions **8** that contain a large excess of internal energy because of the exothermicity, 181.2 kJ mol^{-1}, of their formation process. The experimental results are consistent with the theoretically computed structure of the product, in that the CAD spectrum of the $C_2H_3NXe^+$ population from reaction 9, displaying only the Xe^+ fragment, is consistent with the $H_3C-C-N-Xe^+$ connectivity of **9** and the reactive probing experiments characterize the $C_2H_3NXe^+$ ions from 9 as Xe^+ donors, as expected for species **9**.

Interestingly, the gas-phase reaction sequence leading to Xe^+ transfer finds a close analogy with the sequence established by mechanistic studies in solution, e.g., the reaction

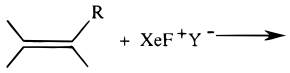

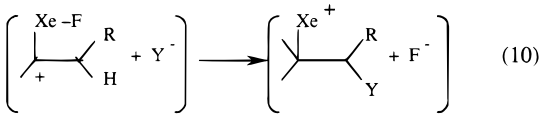

(10)

which eventually yields a cis-fluorinated product and obeys Markovnikov regioselectivity.[2d]

Conclusions

To the best of our knowledge, this study affords the first example of the two-fold reactivity of the gaseous XeF^+ electrophile toward a model substrate, demonstrating its ability to transfer either F^+ or Xe^+ to the N atom of acetonitrile.

Furthermore, the mutual supporting results of mass spectrometric and theoretical methods has allowed structural and thermochemical characterization of the reaction products. The primary fluorinated product is assigned the H_3C-CNF^+ structure **1**, which represents a local minimum on the [C_2, H_3, N, F]$^+$ potential energy surface. Its rearrangement into the more stable N-protonated fluoroacetonitrile isomer **5**, of $H_2FC-C-N-H$ connectivity, requires that a sizable energy barrier be overcome. The product from Xe^+ transfer is ion **9**, characterized by $H_3C-C-N-Xe^+$ connectivity. Ions **1** and **9** react with selected mucleophiles as F^+ and Xe^+ donors, respectively, according to processes whose products and energetics have been examined by both experimental and theoretical methods.

Experimental Section

All chemicals were research-grade products from Aldrich Chemical Co. and were used without further purification. The gases were obtained from Matheson Gas Products Inc., with a stated purity in excess of 99.95 mol %. The details of the triple quadrupole experiments have been reported in ref 4. Briefly, a VG Micromass Model Quattro spectrometer was used. The ions, generated in the CI source operated at 150 °C and 0.1 Torr, and mass selected in the first quadrupole, were driven into the second quadrupole, actually an RF-only hexapole, containing the neutral reagent whose pressure was adjusted from 4×10^{-6} to 5×10^{-5} Torr, as measured by an ionization gauge. The ion−molecule reactions were investigated at nominal collision energies of 0 eV, whereas the CAD spectra were recorded utilizing Ar as the collider at pressures up to 1.5×10^{-5} Torr and collision energies up to 162 eV (laboratory frame). The charged products were analyzed with the third quadruple scanned at a frequency of 150 amu s^{-1}, accumulating at least 10^2 scans per run.

Acknowledgment. The work performed with the financial support of the Universities "La Sapienza" and "Tor Vergata" of Rome and the University of Perugia, Ministero dell'Università e della Ricerca Scientifica e Tecnologica (MURST), and Consiglio Nazionale delle Ricerche (CNR). The authors express their gratitude to Mr. Giuseppe D'Arcangelo and Dr. Andrea Roselletti, who performed the TQ measurements and the calculations, respectively.

References and Notes

(1) (a) Edwards, A. J.; Halloway, J. H.; Peacock, R. D. *Proc. Chem. Soc.* **1963**, 275. (b) Cohen, B.; Peacock, R. D. *J. Inorg. Nucl. Chem.* **1966**, *28*, 3056. (c) Sladky, F. O.; Bulliner, P. A.; Bastlett, N.; De Boer, B. G.; Zalkin, A. *Chem. Commun.* **1968**, 1048. (d) Bartlett, N.; Gennis, M.; Gilber, D. D.; Morrel, B. K.; Zalkin, A. *Inorg. Chem.* **1973**, *12*, 1717.

(2) (a) Shieh, T. C.; Feit, E. D.; Chernick, C. C.; Yang, N. C. *J. Org. Chem.* **1970**, *35*, 4020. (b) Filler, R. *Isr. J. Chem.* **1978**, *17*, 71. (c) Shellhamer, D. F.; Carter, S. L.; Dunham, R. H.; Stuart, N. G.; Graham, N. G.; Spitsbergen, M. P.; Heasley, Y. L.; Chapman, R. D.; Druelinger, M. L. *J. Chem. Soc., Perkin Trans. 2* **1989**, 159. (d) Zefirov, N. J.; Gakh, A. A.; Zhdankin, V. V.; Stang, P. J. *J. Org. Chem.* **1991**, *56*, 1416.

(3) Bernardi, F.; Cacace, F.; de Petris, G.; Pepi, F.; Rossi, I. *J. Phys. Chem. A* **1998**, *102*, 5831.

(4) Attinà, M.; Bernardi, F.; Cacace, F.; Rossi, I. *Chem. Eur. J.* **1999**, *5*, 1186.

(5) (a) Arnold, F.; Böhringer, H.; Henschen, G. *Geophys. Res. Lett.* **1978**, *5*, 653. (b) Arijs, E.; Nevejans, D.; Ingels, J. *Nature (London)* **1980**, *288*, 684. (c) Arnold, F.; Henschen, G.; Ferguson, E. E. *Planet. Space Sci.* **1981**, *29*, 185.

(6) (a) Becker, K. H.; Jonescu, A. *Geophys. Res. Lett.* **1982**, *9*, 1349. (b) Snider, J. R.; Dawson, G. A. *Geophys. Res. Lett.* **1984**, *11*, 241.

(7) (a) Solomon, P. M.; Jefferts, K. B.; Penzias, A. A.; Wilson, R. W. *Astrophys. J. Lett.* **1971**, *168*, 107. (b) Solomon, P. M.; Penzias, A. A.; Jefferts, K. B.; Wilson, R. W. *Astrophys. J. Lett.* **1973**, *185*, 63. (c) Lovas, F. J.; Johnson, D. R.; Buhl, D.; Snyder, L. E. *Astrophys. J.* **1976**, *209*, 770. (d) Ulich, B. L.; Conklin, E. K. *Nature* **1974**, *240*, 121. (e) Linke, R. A.;

Cummins, S. E.; Green, S.; Thaddeus, P. In *Regions of Recent Star Formation*; Roger, R. S., Dewdney, P. E., Eds.; Reidel: Dortrecht, Germany, 1982; p 391.

(8) Matthews, H. E.; Sears, T. J. *Astrophys. J. Lett*. **1983**, *267*, 53.

(9) (a) Böhringer, H.; Arnold, F. *Nature (London)* **1981**, *290*, 321. (b) Brasseur, G.; Chatel, A. *Ann. Geophys*. **1983**, *1*, 173. (c) Brasseur, G.; Arjis, E.; De Rudder, A.; Nevejaus, D.; Ingels, J. *Geophys. Res. Lett.* **1983**, *10*, 725. (d) Brasseur, G.; Zellner, R.; De Rudder, A.; Arjis, E. *Geophys. Res. Lett.* **1985**, *12*, 117. (e) Arjis, A.; Brasseur, G. J. *Geophys. Res.* **1986**, *91*, 4003.

(10) (a) Herbst, E.; Klemperer, W. *Astrophys. J*. **1973**, *185*, 505. (b) Huntress, W. T., Jr.; Anicich, V. G. *Astrophys. J.* **1976**, *208*, 237. (c) Schiff, H. J.; Bohme, D. K. *Astrophys. J.* **1979**, *232*, 740. (d) De Frees, D. J.; McLean, A. D.; Herbst, E. *Astrophys. J.* **1985**, *293*, 236.

(11) Becke, A. D. *J. Chem. Phys.* **1993**, *98*, 5648.

(12) Stevens, P. J.; Devlin, F. J.; Chablowski, C. F.; Frish, M. J. *J. Phys. Chem.* **1994**, *98*, 11623.

(13) Bartlett, R. J. *Annu. Rev. Phys. Chem.* **1981**, *32*, 359.

(14) Raghavachari, K.; Trucks, G. W.; Pople, J. A.; Head-Gordon, M. *Chem. Phys. Lett.* **1989**, *157*, 479.

(15) (a) Peng, C.; Schlegel, H. B. *Isr. J. Chem.* **1993**, *33*, 449. (b) Peng, C.; Ayala, P. Y.; Schlegel, H. B.; Frisch, M. J. *J. Comput. Chem.* **1996**, *17*, 49.

(16) Frisch, M. J.; Pople, J. A.; Binkley, J. S. *J. Chem. Phys.* **1984**, *80*, 3265.

(17) LaJohn, L. A.; Christiansen, P. A.; Ross, R. B.; Atashroo, T.; Ermler, W. C. *J. Chem. Phys.* **1987**, *87*, 2812.

(18) Pettersson, M.; Lundell, J.; Rasanen, M. *Eur. J. Inorg. Chem.* **1999**, *729*, and references therein.

(19) Frisch, M. J.; Trucks, G. W.; Schlegel, H. B.; Scuseria G. E.; Robb, M. A.; Cheeseman, J. R.; Zakrzewski, V. G.; Montgomery, J. A., Jr.; Stratmann, R. E.; Burant, J. C.; Dapprich, S.; Millam, J. M.; Daniels, A. D.; Kudin, K. N.; Strain, M. C.; Farkas, O.; Tomasi, J.; Barone, V.; Cossi, M.; Cammi, R.; Mennucci, B.; Pomelli, C.; Adamo, C.; Clifford, S.; Ochterski, J.; Petersson, G. A.; Ayala, P. Y.; Cui, Q.; Morokuma, K.; Malick, D. K.; Rabuck, A. D.; Raghavachari, K.; Foresman, J. B.; Cioslowski, J.; Ortiz, J. V.; Stefanov, B. B.; Liu, G.; Liashenko, A.; Piskorz, P., Komaromi, I.; Gomperts, R.; Martin, R. L.; Fox, D. J.; Keith, T.; Al-Laham, M. A.; Peng, C. Y.; Nanayakkara, A.; Gonzales, C.; Challacombe, M.; Gill, P. M. W.; Johnson, B. G.; Chen, W.; Wong, M. W.; Andres, J. L.; Head-Gordon, M.; Replogle, E. S.; Pople, J. A. *Gaussian 98*, revision A.7; Gaussian, Inc., Pittsburgh, PA, 1998.

(20) The optimized geometrical parameters of the species of interest are available from the authors on request.